ORIGINAL PAPER

Size-Dependent Behaviour of Hard Rock Under Triaxial Loading

Manuel A. González-Fernández[1] · Xian Estévez-Ventosa[1] · Leandro R. Alejano[1] · Hossein Masoumi[2]

Abstract

Understanding size effects is important to rigorously analyse the behaviour of rocks and rock masses at different scales and for different applications. A number of empirical and numerical studies have included size effects on the uniaxial compressive strength of different rocks, but only few have focussed on the triaxial compressive strength. In this study, several triaxial tests were conducted on granite samples at different confinements (from 0.2 to 15 MPa) and sizes (from 30 to 84 mm in diameter). The most relevant strength parameters were recovered including peak and residual strengths, orientation and frictional response of shear bands. Size effects were observed to be less dominant at high confining pressures for both peak and residual strengths. The resulting data were analysed in the context of size-dependent rock strength theories. For peak strength analyses, the unified size effect law (USEL) and the improved unified size law (IUSEL) were used, in which the double trends, ascending descending behaviours were observed. Size-dependent Hoek–Brown modified failure criteria based on USEL and IUSEL were fit to peak strengths exhibiting a good agreement between the models and the laboratory data. The brittle-ductile transition and the frictional behaviour of shear band under triaxial loading were also analysed. A clear brittle behaviour was particularly observed in samples with large-diameters tested at low confinements. Finally, in regards to frictional behaviour, the shear band angle found to be affected by both confinement and sample size.

Highlights

- Triaxial tests were conducted on granite samples at different confinements (0.2 to 15 MPa) and sizes (30 to 84 mm in diameter).
- Size-effect (ascending-descending double trend) was observed on peak strength results.
- USEL–IUSEL size-effect laws and Hoek-Brown modified failure criterion were used to model the strength behaviour.
- Brittle-ductile transition and frictional behaviour related to size-effect were analysed.

List of Symbols

USEL	Unified size effect law
IUSEL	Improved unified size effect law
MSDP	Multiaxial Misses-Schleiner and Drucker-Prager criterion
NX	Core diameter of 54 mm
ASTM	American society for testing and materials
SD	Standard deviation
CV	Coefficient of variance
UCS	Uniaxial compressive strength
SEL	Size effect law
FFSEL	Fractal fracture size effect law
σ_0	Intrinsic strength for the ascending part of USEL
d	Sample size in USEL
λ	Dimensionless material parameter in USEL
d_0	Maximum aggregate size of a characteristic sample size in USEL
D_f	Fractal dimension of fracture in USEL
B	Dimensionless material parameter in USEL
f_t	Characteristic strength for the descending part of USEL

✉ Manuel A. González-Fernández
manuel.alejandro.gonzalez.fernandez@uvigo.es

1 CINTECX, GESSMin Group, Department of Natural Resources and Environmental Engineering, University of Vigo, Vigo, Spain

2 Department of Civil Engineering, Monash University, Melbourne, VIC 3800, Australia

MFSL	Multifractal scaling law
MMFSL	Modified multifractal scaling law
f_m	Characteristic strength for the descending part of IUSEL
d	Sample size in IUSEL
l	Material constant with unit of length in IUSEL
f_c	Strength of a sample with an infinite size in IUSEL
d_f	Fractal dimension in IUSEL
m	Hoek–Brown constant
σ_{ci}	Uniaxial compressive strength of the intact rock
TI	Transition index from brittle to ductile
β	Shear band angle
FC	Friction coefficient
τ	Shear stress acting on the shear plane
σ_n	Normal stress acting on the shear plane
A	Slope of the normal and shear stresses linear law during the failure
B	Constant of the normal and shear stresses linear law during the failure

1 Introduction

Study of size effect is important in rock engineering particularly for intact rocks where the laboratory data should be extrapolated to the field settings. Size effect has been proven to be an important factor that can influence the mechanical properties of intact rocks. Several studies have included size effect behaviour of intact rocks under various stress conditions. Majority of these have been performed under uniaxial compression (Mogi 1962; Dhir and Sangha 1973; Baecher and Einstein 1981; Hawkins 1998; Thuro et al. 2001a; Yoshinaka et al. 2008; Darlington et al. 2011; Masoumi et al. 2012, 2014, 2016; Masoumi 2013; Roshan et al. 2017; Quiñones et al. 2017), some under point loading (Broch and Franklin 1972; Bieniawski 1975; Brook 1977, 1980, 1985; Wijk 1980; Greminger 1982; Hawkins 1998; Thuro et al. 2001b; Masoumi et al. 2012, 2018; Forbes et al. 2015) and few under tensile testing (Wijk 1980; Andreev 1991a,b; Butenuth 1997; Thuro et al. 2001b; Çanakcia and Pala 2007; Masoumi et al. 2018). Despite extensive studies in this area, few works included the size effect under triaxial condition, focussing mainly on sedimentary rocks (Singh and Huck 1972; Hunt 1973; Medhurst and Brown 1998; Aubertin et al. 2000; Roshan et al. 2017; Masoumi et al. 2017a) and only one study under limited testing conditions was conducted on hard rock by Walton (2018). This could be due to the complexity associated with the triaxial testing on intact brittle (or quasi-brittle) materials. Such a testing is important as most of the design analyses on rock and rock-like materials are performed based on well-known Mohr–Coulomb (Mohr 1900) or Hoek and Brown (H-B) (1997) criteria where the estimation of cohesion (C) and friction angle (ϕ) as well as H-B parameters are essential. It is noteworthy that the brittleness in materials such as rock is relative to the stiffness of them versus stiffness of the loading frame. Therefore, in this study the referral to "brittle" or "ductile" behaviour is indeed associated with the type of loading frame used in the testing program. Our loading frame can be considered as the type with highest stiffness that are commercially available in the market.

The need to extrapolate the results obtained from the laboratory to a larger size has led to the development of three main size effect theories for intact rocks. The first is based on the statistical distribution of micro-cracks within an intact rock following Weibull (1939) statistical function. The second theory was proposed by Bazant (1984) which relies on the fracture energy concept. The third one was suggested by Carpinteri et al. (1995) based on multifractal scaling concept. It is noteworthy that a number of empirical size effect models have been developed implicitly based on Weibull (1939) statistical theory (e.g. Hoek and Brown 1980; Brook 1980, 1985 and Darlington et al. 2011). From these size effect models, different size-dependent failure criteria have been proposed such as the one by Hoek and Brown (1997) through including an empirical size effect function into their well-known failure criterion. Later, Medhurst and Brown (1998) assessed the predictability of Hoek and Brown size-dependent failure criterion on a number of coal samples with different sizes and at various confining pressures. A comprehensive triaxial size effect criterion was proposed by Aubertin et al. (2000) in which the size effect parameter was included into MSDP (Multiaxial Misses-Schleiner and Drucker-Prager criterion). Masoumi et al. (2017a) suggested a methodology to include the unified size effect law (USEL) (Masoumi et al. 2016) into Hoek and Brown failure criterion and assessed its performance based on the triaxial data obtained from Gosford sandstone.

The genesis of USEL originated from Hawkins (1998) study who conducted an extensive set of laboratory tests on different sedimentary rocks and demonstrated that the uniaxial compressive strengths (UCS) of these rocks at different sizes follow an ascending and then descending trend. At about the same time, Bazant (1997) developed a fractal fracture size effect model to capture such an ascending and then descending behaviour. Masoumi (2013) and Masoumi et al. (2016) extensively investigated such a phenomenon for a particular sandstone, as well as those investigated by Hawkins (1998) and explained that such a strength ascending and then descending behaviour can be associated with the effect of end surface flaws, which are dominant in the samples with small diameters and also the fractal characteristics of rocks. These two physical theories were then supplemented by USEL proposed by Masoumi et al. (2016). Later, such a

phenomenon was endorsed by Quiñones et al. (2017) who also reported such a strength ascending and then descending trend on Blanco Mera granite under uniaxial compression as a first study on hard rock samples. In another study, Masoumi et al. (2017a) demonstrated the applicability of strength ascending and then descending trend to Gosford sandstone under triaxial condition, which all were explained based on the two physical theories highlighted earlier including end surface flaws effect and fractality. Zhai et al. (2020) also demonstrated that the strength ascending and descending behaviour is applicable to weak rocks, including Gambier limestone and a synthetic gypsum material with UCS of less than 10 MPa.

The sample size not only affect the elastic and strength properties of an intact rock, it can also impact the overall mechanical behaviour of rock under loading such as transition from brittle to ductile behaviour and formation of shear band particularly under triaxial condition (Roshan et al. 2017). Therefore, it is relevant to advance towards extensive assessment of size effect models for different rocks, in particular those which have been limitedly examined such as hard rocks. To contribute to this endeavour, a dedicated laboratory program was developed to extend the current knowledge gap on size effect behaviour of hard rock under triaxial condition (Arzúa and Alejano 2013; Quiñones et al. 2017; Alejano et al. 2021). As a result, about 100 triaxial compressive tests were performed on Blanco Mera granite at four different diameters including 30, 38, 54 and 84 mm using a set of specially tailored Hoek cells. The triaxial tests were conducted between 0.2 and 15 MPa confining pressures. The resulting shear band orientations at different sizes and confinements were measured and compared along with the transition from brittle to ductile behaviour due to change in size and confining pressure. The strength ascending and then descending trends of granite samples were examined based on USEL and its improved version (IUSEL) and then, their fitability to Hoek and Brown criterion were assessed. Finally, it was concluded that the size-dependent Hoek–Brown failure criterion can accurately capture the strength behaviours of Blanco Mera granite.

2 Experimental Work

2.1 Rock Sample Selection and Preparation

The Blanco Mera granite used in this study was supplied from the province of Lugo in Spain. Arzúa and Alejano (2013), Arzúa et al. (2014) and Alejano et al. (2017) performed different mechanical studies on Blanco Mera granite which is a bright white-coloured granite that consists of 35% plagioclase feldspar, 27% alkali feldspar, 20% quartz, 7% muscovite, 5% biotite and other minerals at below 5%

including chlorite and sericite. The grain distribution in this granite, to some extent is scattered as shown in Fig. 1a where the size of quartz crystals ranges from 1 to 6 mm and feldspar crystals from 1 to 3 mm along with various mica minerals.

About 100 core samples were prepared at diameters of 30, 38, 54 (NX) and 84 mm (see Fig. 1b and c). The length to diameter ratio of the samples was about 2 complying with ASTM (2014) and ISRM (2007) recommendations which was also suitable to be used in Hoek cell. A number of Hoek cells at different sizes (see Fig. 1d) were designed
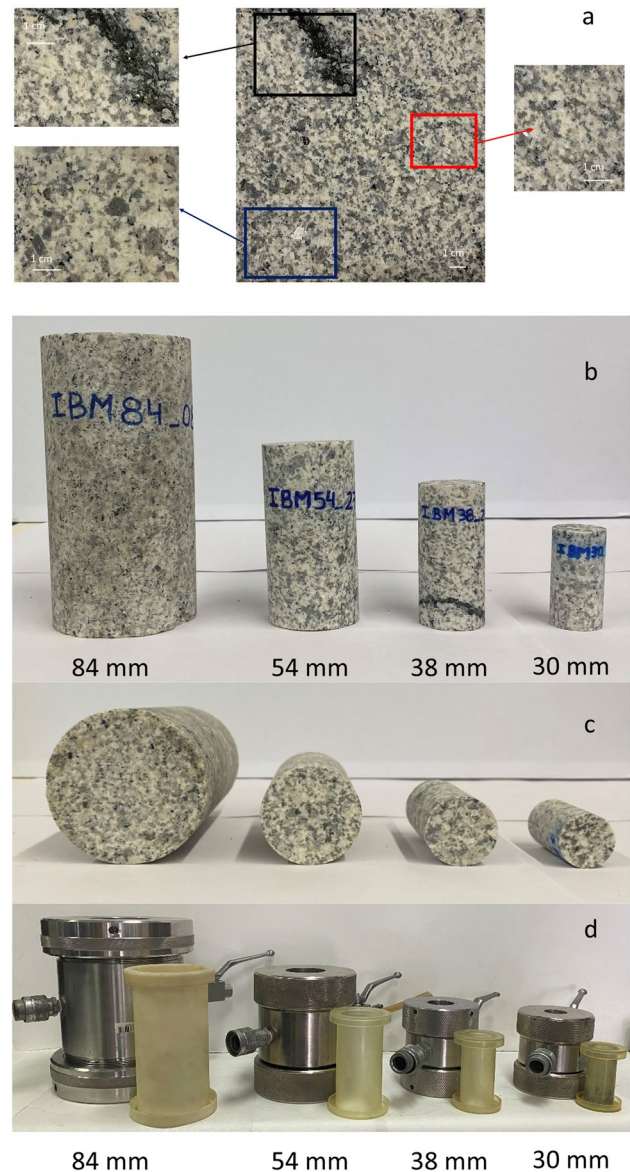
Fig. 1 **a** 15×15 cm^2 digital photo of the surface of Blanco Mera granite at the centre along with digital photos with $3 \times$ zoom from different areas to highlight its heterogeneity. Samples with different diameters showing **b** side and **c** top views as well as **d** the designed and fabricated Hoek cells along with their sleeves for various sizes

Table 1 The number of triaxial tests conducted at various diameters and confining pressures

| Confining pressure (MPa)	Diameter (mm)			
	30	38	54	84
0.2	4	4	4	4
2.5	2	3	3	3
5.0	4	4	4	4
7.5	3	3	3	3
10.0	4	4	4	4
12.5	2	3	2	3
15.0	4	4	4	4

and fabricated to perform a suite of triaxial experiments on granite samples with various sizes and confinements (e.g. 0.2, 2.5, 5, 7.5, 10, 12.5 and 15 MPa). To account for variability in data, a number of repetitions was performed at different diameters and confining pressures as listed in Table 1.

2.2 Testing Procedure

To perform the triaxial tests, a 200 tonne servo-controlled loading frame was used as shown in Fig. 2a. The testing system consisted of a load frame where the Hoek cell was fitted into its central part, the extensometers which were mounted to the Hoek cells, the hydraulic pumps to control the confining pressure, test controller and a computer for data acquisition. Strain gauges were used inside the Hoek cell which were attached to the samples for axial and radial strains measurement as demonstrated in Fig. 2b. The frame movement was also measured axially using Linear Variable Differential Transducer (LVDT). Water was used as a fluid to supply confining pressure and its volumetric changes were measured to report sample volumetric strain which is useful to study the post-failure response.

2.3 Test Results

Extensive laboratory data were extracted from the triaxial experiments including peak and residual strengths, elastic limit (derived from gauge measurements) and shear band angles. A typical representation of the data obtained from the tests is shown in Fig. 3. This figure demonstrates the stress–strain curves obtained from the axial and radial strain gauges, the axial strain recorded by LVDTs and the volumetric strain. The peak strength was the maximum stress recorded during the test and the residual strength was calculated as the value of stress towards the end of the experiment where an increase in the strain does not cause any significant (e.g. less than 1 MPa) change in the stress. The elastic limit was calculated from the linear section of the stress–strain curve, using the data collected by the strain gauges where the linear part lies at about 50% peak strength. The average
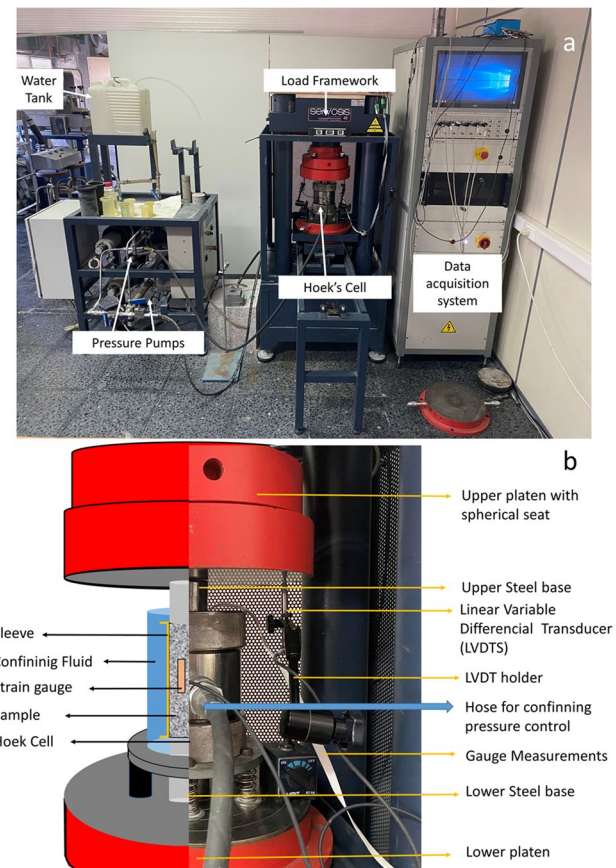

Fig. 2 a General view of the testing system used for the triaxial experiments. **b** Schematic representation of the interior of a Hoek cell

of the resulting peak and residual strengths, elastic limits and shear band angles at different confinements and diameters are presented in Table 2. The resulting stress–strain curves obtained from the sample with 38 mm diameter at various confinements along with the triaxial tests under 0.2 MPa confining pressures on samples with 30, 38, 54 and 84 mm diameters are presented in Fig. 4.

The shear band angle β was defined as the angle between the shear band and the horizontal line as shown in Fig. 5. It is worth remarking the impossibility of measurement of such an angle for almost all samples tested under 0.2 MPa confining pressure due to complex failure patterns which tend to include a number of tensile cracks with no or little shearing as depicted in Fig. 5. Also, all failed samples with 30 mm diameter are shown in Fig. 6. The resulting failure patterns under low confining pressures are mainly axial splitting with a transition to shear band failure mechanism at high confinements.

The peak strengths obtained from various diameters and confining pressures were plotted and compared in Fig. 7a. It is clear that an increase in the confining pressure led to a rise in the peak strengths, where an ascending and then

Fig. 3 Example of stress–strain curves obtained from the triaxial test on a sample with the diameter of 38 mm tested at 12.5 MPa confinement
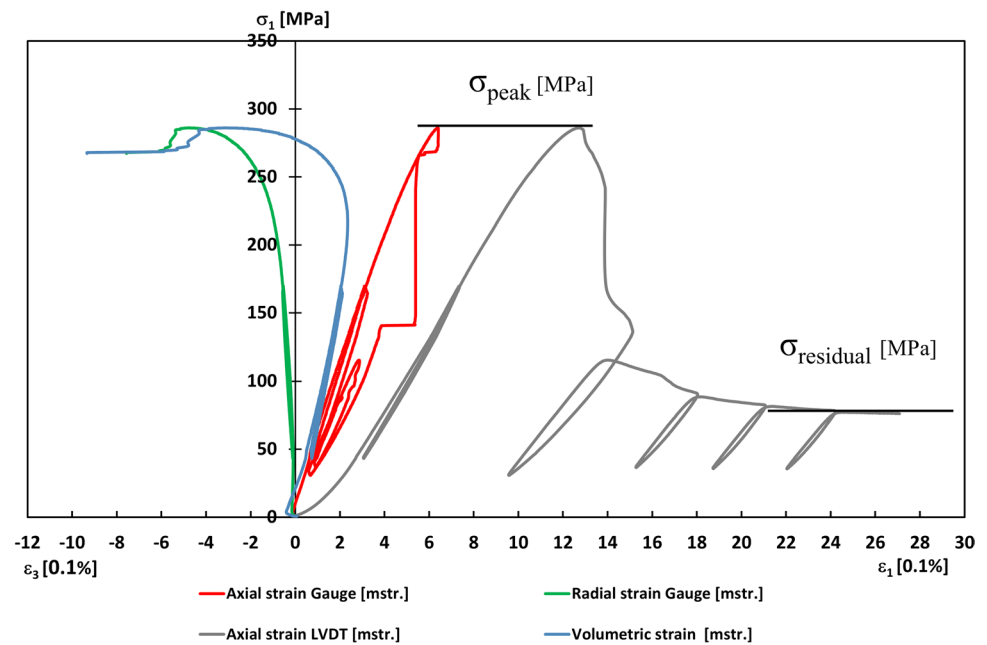
descending trend is observable at almost all confining pressures due to change in sample diameter which can be associated with end surface flaws effect as well as fractal characteristics of Blanco Mera granite according to Masoumi et al. (2016).

It is believed that at 5 MPa confinement, rock heterogeneity was the main factor that such a trend was not clearly visible compared to other confining pressures. From these data, two trends can be deduced. At low confining pressures (less than 5 MPa), there is a clear size effect behaviour as that reported by Masoumi (2013) and Quiñones et al. (2017) where the strength increases from small sizes up to 54 mm diameter and then decreases at larger diameters. At higher confinements (between 5 and 10 MPa), such an ascending and then descending trend is not as clear as those observed at low confinements highlighting Aubertin et al. (2000) argument where an increase in confining pressure can lead to less size effect in rock materials. Such an argument is even more recognisable for samples tested at 12.5 and 15 MPa confining pressures. This behaviour was also reported by Gerogiannopoulos and Brown (1978) as well as Michelis (1987) who tested marble. The role of pre-existing micro-cracks in tested granite can be considered as the major factor for controlling the size effect at different confining pressures. It is believed that at low confining pressures the pre-existing micro-cracks control the size effect based on any defined theories such as weakest link by Weibull (1939), fracture energy by Bazant (1984) or multifractality by Carpinteri et al. (1995). However, with an increase in confining pressure, these cracks close and thus less size effect behaviour is expected. Such a finding is quite important from practical viewpoint where the data from the laboratory environment is

extrapolated to the field setting such as a deep underground rock engineering project.

A size effect analysis was also conducted on the residual strengths obtained from various confinements and diameters. Figure 7b illustrates the size effect behaviour of the resulting residual strengths where only at low confinements (less than 5 MPa), the ascending and then descending trends similar to that observed for the peak strengths are recognisable. The lack of significant size effect at the residual strengths was also reported by Archambault et al. (1993), Roshan et al. (2017), Walton (2018) and Alejano et al. (2021) who argued that due to disintegration of rock samples after failure, the defined size effect theories cannot be applicable to residual state.

3 Analytical Study

In this section, various aspects of results relevant to size effects on intact rock are analysed. First the peak strengths at different confinements are analysed in the context of different size effect laws to assess their size dependency in regards to confinement effect. Then, a couple of size-dependent Hoek–Brown failure criteria inspired by the work conducted by Masoumi et al. (2017a) are proposed to examine the reliability of such criteria for Blanco Mera granite.

3.1 Size Effects Laws and Their Fitability

Unified size effect law (USEL) (Masoumi et al. 2016) and its improved version (IUSEL) (Masoumi et al. 2017b) were used to perform size-dependent analysis on peak strength

Table 2 Average of the peak and residual strengths, standard deviation and coefficient of variation for peak and residual strengths, elastic limit and shear band angle obtained from tested samples

Confining pressure (MPa)	Diameter (mm)	Repetition	Average peak strength (MPa)	Peak strength SD (MPa)	Peak strength CV (%)	Average residual strength (MPa)	Residual strength SD (MPa)	Residual strength CV (%)	Mean elastic limit (GPa)	Shear band angle (°)
0.2	30	4	95.41	13.55	14.20	11.75	2.06	17.55	48.9	–
	38	4	119.90	6.36	5.30	18.25	3.30	18.10	51.7	–
	54	4	131.27	17.38	13.24	23.75	10.34	43.54	47.4	–
	84	4	85.80	24.34	28.36	8.75	3.59	41.07	35.1	–
2.5	30	2	117.69	42.59	36.19	24.00	1.41	5.89	49.5	72.00
	38	3	156.82	13.19	8.41	30.00	6.08	20.28	45.9	73.33
	54	3	173.82	27.92	16.06	36.67	4.73	12.89	51.5	73.50
	84	3	142.46	16.08	11.28	29.67	1.53	5.15	50.4	73.33
5	30	4	170.99	21.19	12.39	44.50	7.94	17.84	49.5	67.50
	38	4	177.61	24.82	13.98	46.00	11.52	25.04	50.8	70.00
	54	4	164.38	16.23	9.87	52.50	21.76	41.46	50.1	71.67
	84	4	163.57	17.07	10.44	45.75	9.00	19.66	44.2	70.75
7.5	30	3	176.58	48.06	27.22	62.00	27.06	43.64	53.5	64.00
	38	3	208.87	40.74	19.50	63.33	16.07	25.38	55.4	68.33
	54	3	215.81	27.98	12.96	57.00	10.39	18.23	54.2	67.67
	84	3	213.77	25.26	11.82	61.33	10.69	17.43	50.9	69.33
10	30	4	231.62	19.06	8.23	68.50	12.07	17.62	49.5	62.50
	38	4	243.72	6.75	2.77	68.00	11.52	16.94	56.5	65.75
	54	4	235.14	25.56	10.87	65.00	6.00	9.23	53.8	64.50
	84	4	216.39	18.96	8.76	70.00	8.72	12.45	51.7	67.00
12.5	30	2	255.68	27.52	10.76	81.00	1.41	1.75	51.8	61.50
	38	3	280.84	8.08	2.88	82.00	5.57	6.79	52.7	62.67
	54	2	260.07	10.82	4.16	69.00	5.66	8.20	57.2	64.00
	84	3	239.78	17.78	7.42	76.67	9.87	12.87	52.6	64.33
15	30	4	297.69	9.64	3.24	87.50	13.18	15.06	53.7	58.67
	38	4	293.56	7.05	2.40	89.00	4.83	5.43	58.5	59.25
	54	4	278.08	40.38	14.52	88.50	11.12	12.57	53.0	60.75
	84	4	278.55	27.15	9.75	92.25	4.35	4.71	49.2	61.75
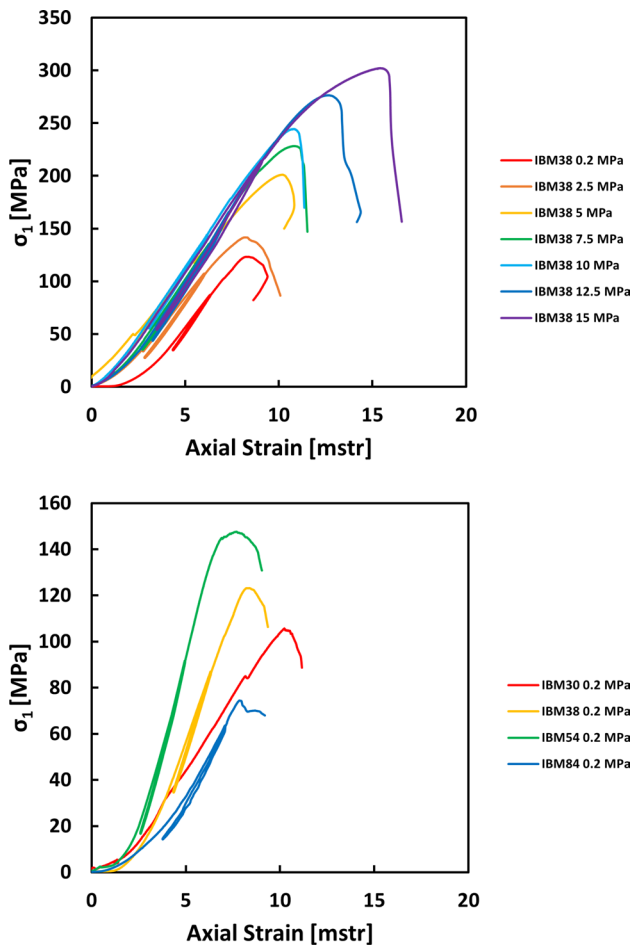
Fig. 4 Stress–strain curves (recorded from LVDT measurements) obtained from samples with 38 mm diameter at various confinements (top) and the triaxial tests at 0.2 MPa confining pressures on samples with 30, 38, 54 and 84 mm diameters (bottom)

data. The resulting trends were also compared so that the predictability of each model can be assessed.

3.1.1 Unified Size Effect Law

Masoumi et al. (2016) proposed the unified size effect law (USEL) to predict the strength ascending and then descending behaviour of intact rocks, particularly sedimentary rocks. USEL consists of two parts including the strength descending behaviour which was explained based on the fracture energy theory according to Bazant (1984) who proposed size effect law (SEL) and the strength ascending behaviour based on fractal fracture size effect law (FFSEL) introduced by Bazant (1997). A combination of SEL and FFSEL was defined as USEL so that the strength at each size is estimated as the minimum value obtained from SEL and FFSEL as follows:

$$\text{Strength} = \min\left(\frac{\sigma_0 d^{(D_f-1)/2}}{\sqrt{1+(d/\lambda d_0)}}(\text{FFSEL}), \frac{Bf_t}{\sqrt{1+(d/\lambda d_0)}}(\text{SEL})\right)$$

(1)

where, σ_0 is the intrinsic or characteristic strength associated with the ascending part, d is the sample size, λ is a dimensional parameter, d_0 is the maximum sample size that can be referred to as a characteristic size and D_f is the fractal dimension related to the fracture surface. It is noteworthy that $D_f = 1$ for non-fractal surfaces and $D_f \neq 1$ for fractal surfaces. In SEL, B is the dimensional parameter and f_t is the intrinsic or characteristic strength.

To calibrate the USEL parameters, first the SEL parameters including Bf_t and λd_0 are estimated through the curve fitting process. Hence, a similar approach is followed to
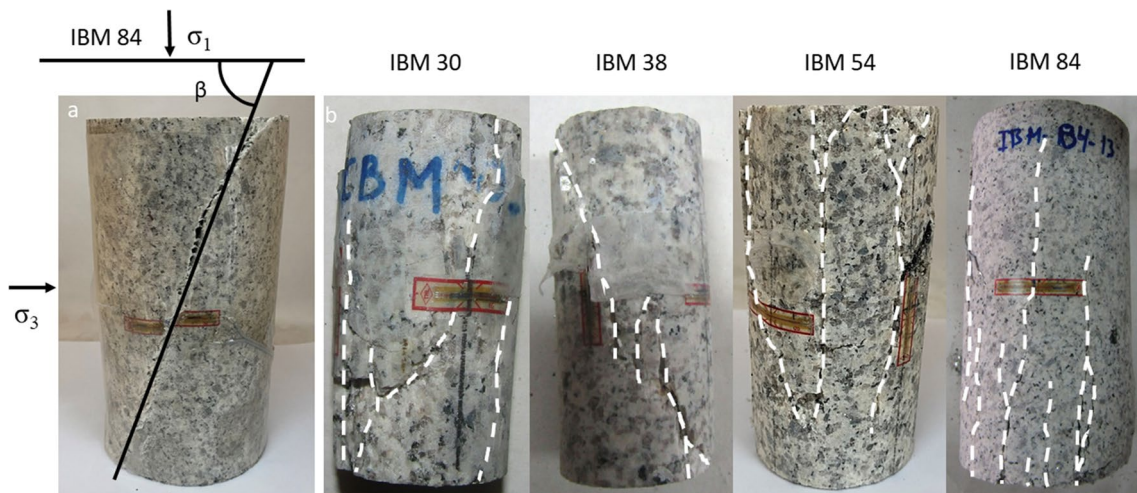
Fig. 5 a Example of an 84 mm diameter sample tested at 12.5 MPa confinement with a clear shear band angle and **b** samples of all sizes tested at 0.2 MPa confining pressure exhibiting axial splitting failure patterns highlighted in white
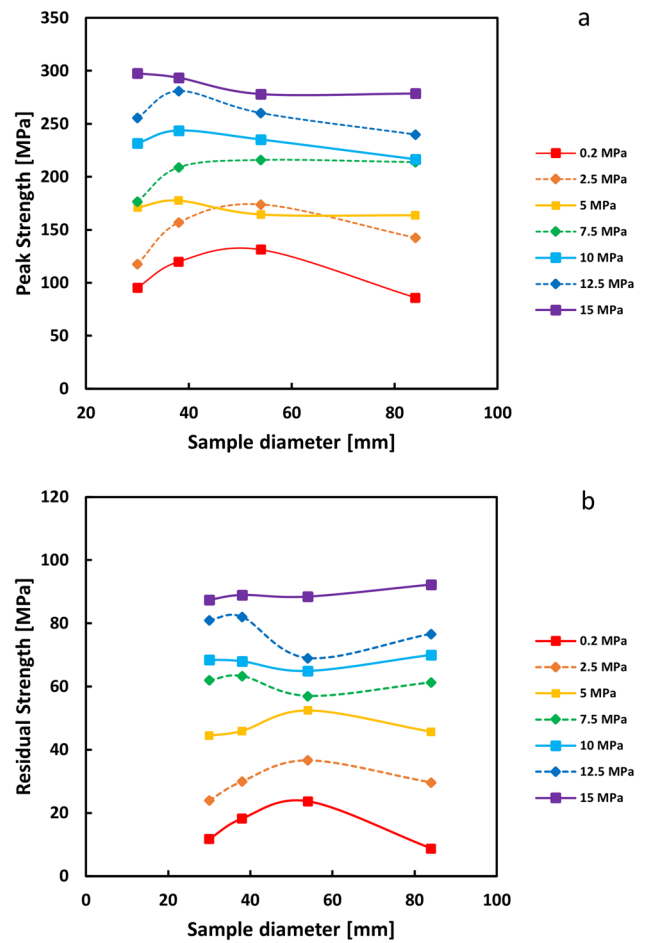
30 mm σ₃ 0.2 MPa   30 mm σ₃ 2.5 MPa

30 mm σ₃ 5 MPa   30 mm σ₃ 7.5 MPa   30 mm σ₃ 10 MPa

30 mm σ₃ 12.5 MPa   30 mm σ₃ 15 MPa
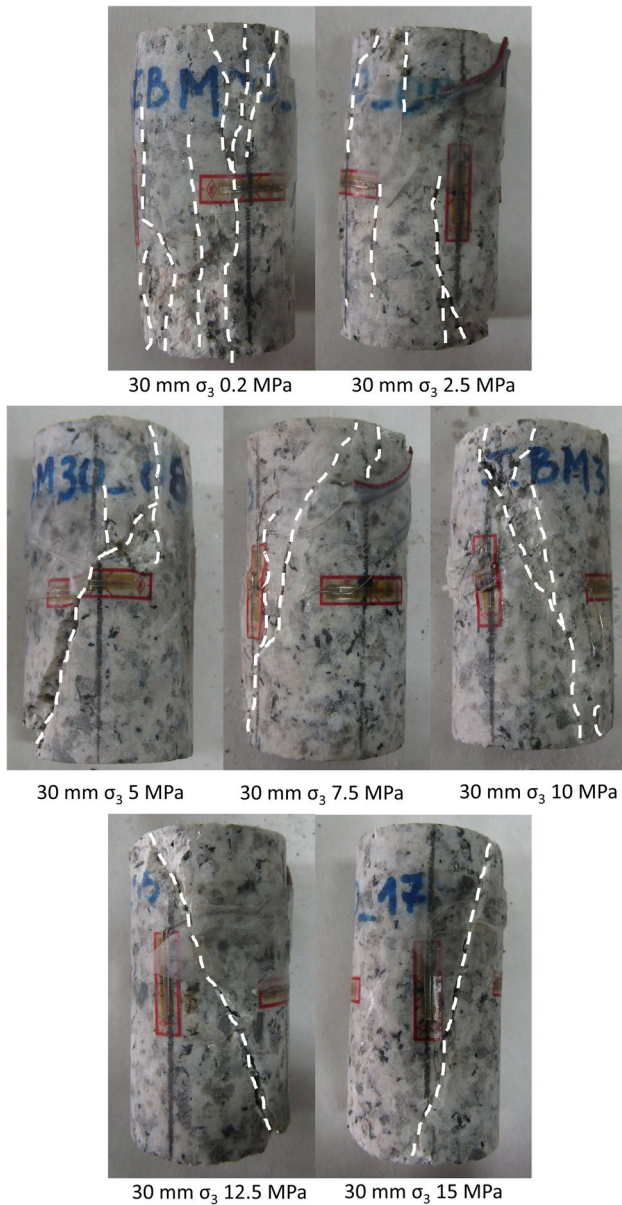
Fig. 6 Failure patterns of samples with 30 mm diameter tested at different confining pressures

Fig. 7 a Size effect behaviour of peak strengths obtained from Blanco Mera granite at various confining pressures. **b** Size effect behaviour of residual strengths obtained from Blanco Mera granite at various confining pressures

obtain the FFSEL parameters being σ_0 and D_f. It should be noted that for those sizes in which $D_f = 1$, Bf_t is equal to σ_0, meaning that the corresponding data will not show fractal characteristics and thus, the FFSEL becomes the same as SEL. The intersection diameter of SEL and FFSEL (D_i) happens according to:

$$D_i = \left(\frac{Bf_t}{\sigma_0} \right)^{2 \big/ (D_f - 1)} \tag{2}$$

and its corresponding strength can be estimated using the following equation:

$$\text{Strength} = \frac{Bf_t}{\sqrt{1 + \left(\left(Bf_t / \sigma_0 \right)^{2 \big/ (D_f - 1)} \Big/ \lambda d_0 \right)}} \tag{3}$$

3.1.2 Improved Unified Size Effect Law

Masoumi et al. (2017b) proposed an improved version of USEL (IUSEL) based on fractality concept. The main advantage of IUSEL versus USEL is its ability to predict a realistic strength for a sample with an infinite size. Such an improvement was developed based on two fractal models in the same vein as that for USEL including ascending and descending parts. The descending part was developed by Carpinteri et al. (1999) known as "multifractal scaling law" or MFSL. The ascending part was developed by Masoumi et al. (2017b) following the same approach as that implemented by Bazant (1997) for FFSEL leading to "modified multifractal scaling

law" or MMFSL. As a result, the combination of MFSL and MMFSL were introduced as IUSEL according to:

$$\text{Strength} = \min\left(f_m d^{(d_f-1)/2} \sqrt{1 + \frac{l}{d}} (\text{MMFSL}), f_c \sqrt{1 + \frac{l}{d}} (\text{MFSL}) \right) \tag{4}$$

where, f_m is a characteristic strength of the ascending zone, d is the sample size, d_f is the fractal dimension, l is a material constant with length unit and f_c is a characteristic strength associated with the descending zone. The calibration process for IUSEL is consistent with that for USEL where the parameters of descending part are estimated first, followed by the ascending part. The diameter at the intersection of MFSL and MMFSL can be estimated using below equation:

$$d_i = \left(\frac{f_c}{f_m} \right)^{2/(d_f-1)} \tag{5}$$

and the strength at the intersection diameter or the maximum strength of Eq. (4) is estimated as follows:

$$\text{Strength} = f_c \sqrt{1 + \frac{l}{\left(\frac{f_c}{f_m} \right)^{2/(d_f-1)}}} \tag{6}$$

3.1.3 Predictability Assessment of USEL and IUSEL on the Triaxial Data with Negligible Confinement

According to Masoumi et al. (2016) and Zhai et al. (2020) three scenarios can be considered for calibration of USEL and IUSEL to the uniaxial compressive strength data or the triaxial data with negligible confinement such as here (0.2 MPa). First, the characteristic diameter with maximum strength is only included in the ascending part, second, it is only included in the descending part and lastly it is included in both ascending and descending parts. All these three scenarios were modelled for both USEL and IUSEL and the resulting parameters are listed in Tables 3 and 4, respectively. Only the ones with the best fit (maximum R^2) which are underlined in Tables 3 and 4 are visualised in Fig. 8. It should be noted that for both USEL and IUSEL, the best fits happened when the maximum strength was included in both ascending and descending parts.

From Fig. 8, it is clear that predictions by both USEL and IUSEL match well with the experimental data. The major improvement in IUSEL is the realistic prediction of the strength of a sample with an infinite size which is highlighted in Fig. 9 where the strength prediction of a granite with very large size at 0.2 MPa confining pressure by IUSEL tends to a constant value while USEL tends to zero.

Table 3 Predicted parameters for USEL based on the triaxial data with 0.2 MPa confinement obtained from Blanco Mera granite

| Confininig pressure (MPa)	Diameter with maximum σ_1 value (mm)	Bf_t (MPa)	λd_0 (mm)	σ_0 (MPa)	d_f	Diameter at intersection (mm)	R^2
Maximum strength included in SEL							
0.2	54	7143	0.02	35.93	3.80	43.65	0.57
Maximum strength included in FFSEL							
0.2	54	85.31	8.53E+09	19.34	1.97	21.26	0.08
Maximum strength included in both SEL and FFSEL							
0.2	54	7145	0.01575	154.2	2.97	49.12	0.60

Underlined values refer to those calculated with the best fit

Table 4 Predicted parameters for IUSEL based on the triaxial data with 0.2 MPa confinement obtained from Blanco Mera granite

Confining Pressure (MPa)	Diameter with maximum σ_1 value (mm)	f_c (MPa)	l (mm)	f_m (MPa)	d_f	Diameter at intersection (mm)	R^2
Maximum strength included in MFSL							
0.2	54	1.591	317,500	0.008	3.80	43.60	0.57
Maximum strength included in MMFSL							
0.2	54	612.1	8.36E+01	–	–	–	–
Maximum strength included in both MFSL and MMFSL							
0.2	54	1.591	3.18E+05	0.03432	2.97	49.15	0.60

Underlined values refer to those calculated with the best fit

Fig. 8 Strengths prediction by USEL and IUSEL for Blanco Mera granite tested under negligible confinement

$\sigma_3 = 0.2$ MPa
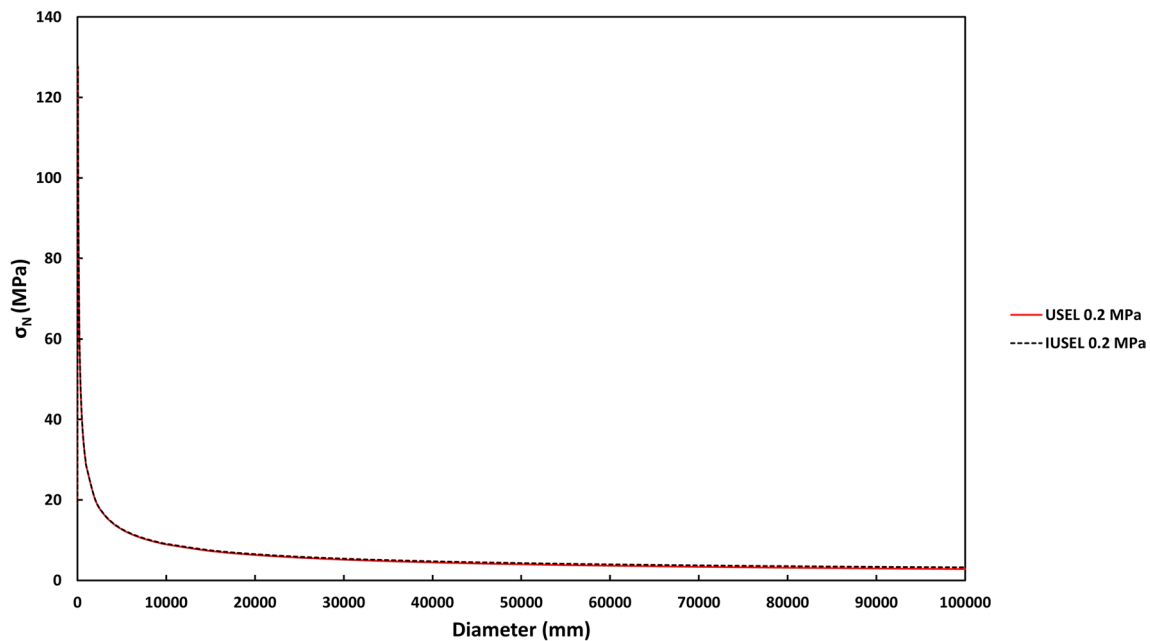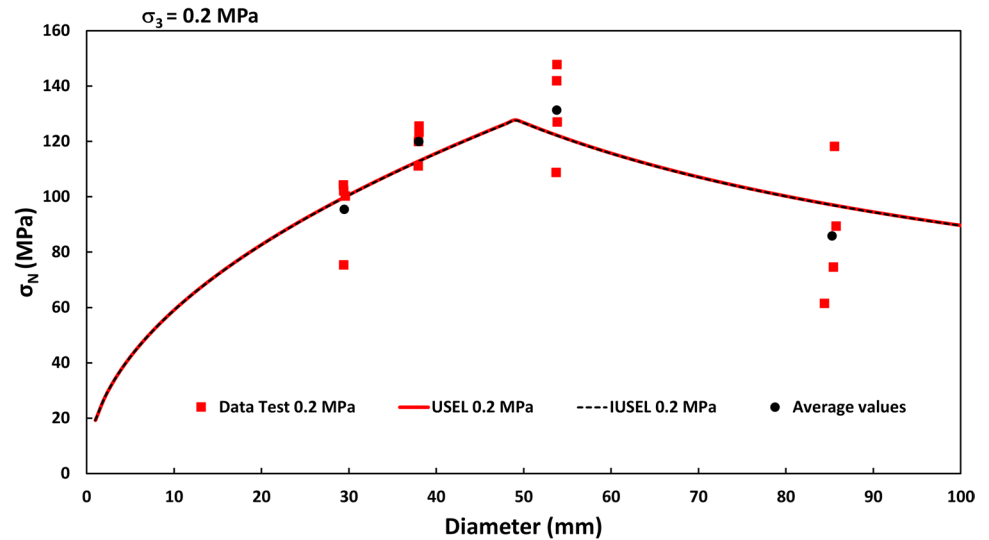
Fig. 9 Prediction assessment by USEL (specifically SEL) and IUSEL (specifically MFSL) for large sizes of granite at negligible confinement

3.2 Size-Dependent Hoek–Brown Failure Criterion

Masoumi et al. (2017a) modified the original and widely used Hoek and Brown (1997) failure criterion for intact rocks by incorporating USEL into it leading to the size-dependent Hoek and Brown failure criterion. In the modified criterion, the uniaxial compressive strength (σ_{ci}) was replaced by USEL resulting in:

$$\sigma_1 = \sigma_3 + \min\left(\frac{\sigma_0 d^{(D_f-1)/2}}{\sqrt{1+(d/\lambda d_0)}}, \frac{Bf_t}{\sqrt{1+(d/\lambda d_0)}}\right) \times \left(m\frac{\sigma_3}{\min\left(\frac{\sigma_0 d^{(D_f-1)/2}}{\sqrt{1+(d/\lambda d_0)}}, \frac{Bf_t}{\sqrt{1+(d/\lambda d_0)}}\right)} + 1\right)^{0.5} \qquad (7)$$

where, σ_1 is the axial stress, σ_3 is the confining pressure and m is the Hoek and Brown constant that controls the curvature of the criterion. The rest of the parameters were defined earlier when USEL was presented. The improved version of USEL was proposed by Masoumi et al. (2017b) and here the IUSEL is incorporated into Hoek and Brown failure criterion in the same vein as that considered by Masoumi et al. (2017a) leading to:

$$\sigma_1 = \sigma_3 + \min\left(f_m d^{(d_f-1)/2}\sqrt{1+\frac{l}{d}}, f_c\sqrt{1+\frac{l}{d}}\right)$$
$$\times \left(m\frac{\sigma_3}{\min\left(f_m d^{(d_f-1)/2}\sqrt{1+\frac{l}{d}}, f_c\sqrt{1+\frac{l}{d}}\right)} + 1\right)^{0.5}$$
$$(8)$$

where, all the parameters were already defined. For models calibration, a wide range of data sets at different confinements and diameters are required so that the USEL and IUSEL parameters can be calibrated based on the data obtained under uniaxial compression (or in our case under triaxial condition with negligible confining pressure). Hence, m is calibrated for each sample size tested at various confining pressures and then the average of m values obtained from

different diameters is used to visualise the three-dimensional graph of axial stress-confining pressure-sample size.

As a result, the USEL and IUSEL parameters (see Tables 3 and 4) that were calibrated earlier for the samples with different diameters tested under 0.2 MPa confinement were used to estimate the remaining parameters of size-dependent Hoek and Brown models as listed in Table 5. It is noteworthy that σ_{ci} in Table 5 for USEL and IUSEL is the strength prediction for each diameter based on USEL and IUSEL and the resulting m_i for each diameter obtained from the curve fitting.

The size-dependent Hoek–Brown failure criteria based on USEL and IUSEL are presented in Fig. 10.

The resulting values for the parameters of size-dependent Hoek–Brown failure criteria based on USEL and ISUEL found to be very close and thus, the deriving fits from these parameters depicted on Fig. 10 are overlapped. It is noteworthy that the predictions by both models match well with the experimental data. It is also worth mentioning that based on the modelling analysis, it was concluded that m parameter to high extent seem to be size independent as the resulting m values from different diameters are close to each other. Such a size independent characteristic can be further explored for different rocks based on more laboratory triaxial experiments on rocks with various sizes.

4 Brittle–Ductile Transition and Frictional Behaviours

In this section, the potential size dependency of the brittle-ductile transition and the frictional behaviour of Blanco Mera granite due to increase in confining pressure are investigated.

4.1 Size Effects on Brittle-Ductile Transition

It has been proven that rocks show a transition from brittle to ductile behaviour due to an increase in the confining stress (Mogi 1966; Brady and Brown 2006). Some studies have linked this behaviour to the closure of non-critical microfractures as the confining pressure is increased (Wawersik and Fairhurst 1970; Elliot and Brown 1985). Others have
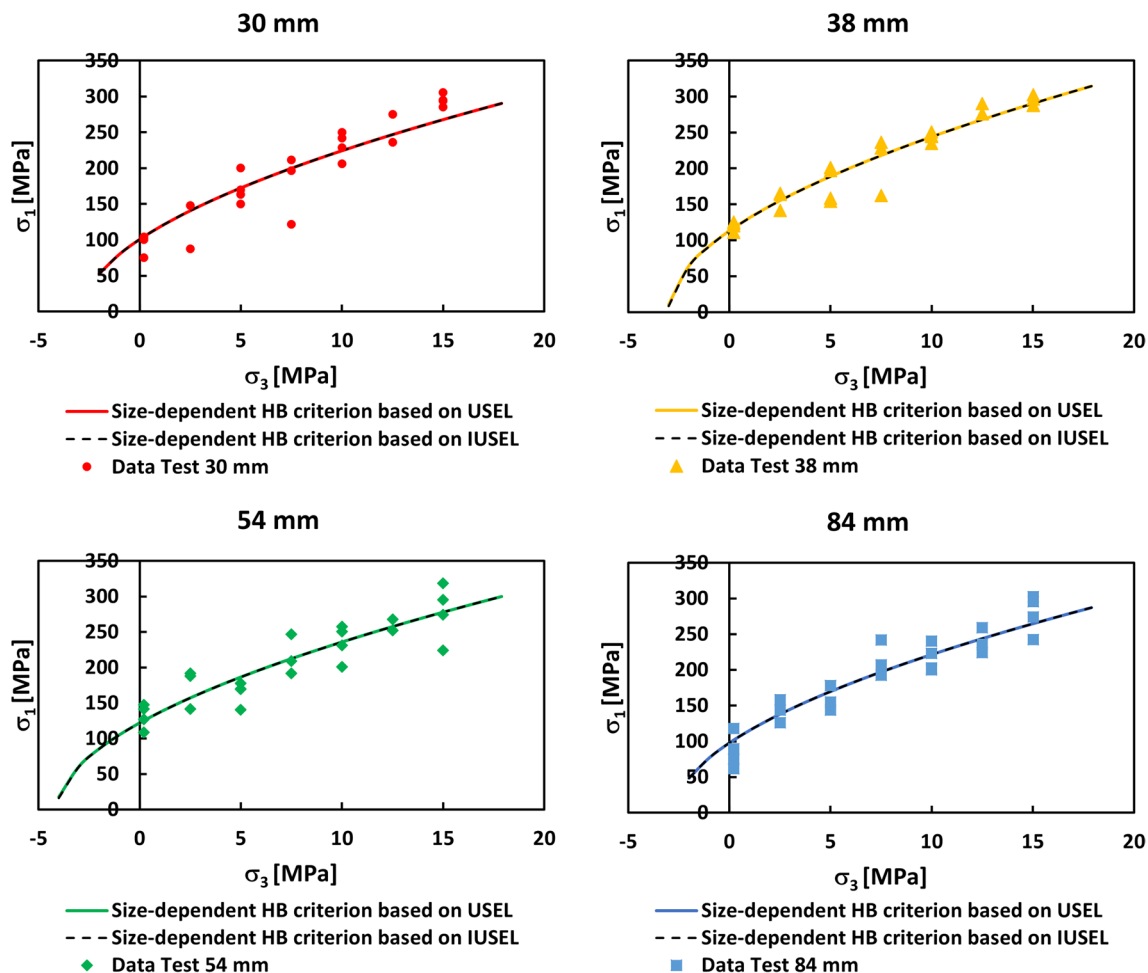
Table 5 The resulting Hoek–Brown parameters for size-dependent failure criteria based on USEL and IUSEL

Diameter (mm)	Parameter	H-B based on USEL	H-B based on IUSEL
30	m	35.50	35.58
	σ_{ci} (MPa)	100.70	100.58
	R^2	0.89	0.89
38	m	37.13	37.13
	σ_{ci} (MPa)	112.94	112.80
	R^2	0.93	0.93
54	m	29.55	29.65
	σ_{ci} (MPa)	122.10	121.91
	R^2	0.80	0.80
84	m	35.91	35.97
	σ_{ci} (MPa)	97.83	97.75
	R^2	0.90	0.90

Fig. 10 Size-dependent Hoek–Brown predictions for Blanco Mera granite samples based on USEL and IUSEL for different sample sizes

identified the type of micro-failure mechanism at stake being responsible for such a transition (Griffith 1921; Martin and Chandler 1994; Diederichs 2007) where tensile failure associated with micro-cracks propagation and coalescence tends to produce a more brittle response while the shear failure at typically large sizes and high confinements induce more ductile behaviour. Certainly, both reasons can contribute to the transition from brittle to ductile behaviour.

While the effects of confining pressure on brittle to ductile transition have been widely studied for different rock types (Edmond and Paterson 1972; Barton 1976; Shah 1997; Walton et al. 2017; Bruning et al. 2019), very limited studies (e.g. Roshan et al. 2017) have analysed the size dependency of such a transition. According to Roshan et al. (2017), the transition from brittle to ductile behaviour can be defined as a non-dimensional transition index (TI) which is the difference between the mean peak and residual strengths at different confining pressures and is normalized with the mean peak strength as follows:
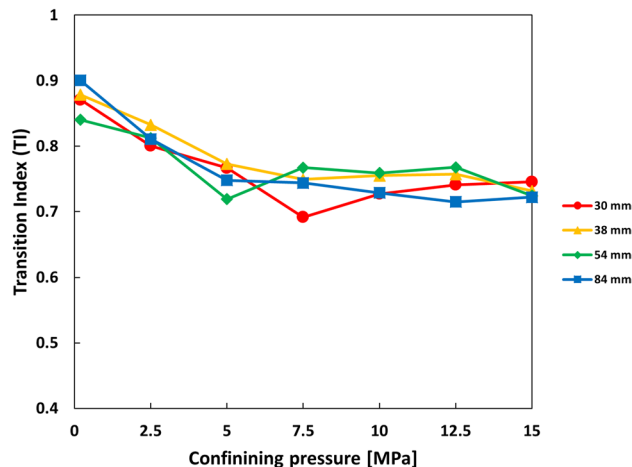
Fig. 11 Transition index (TI) versus confining pressure for Blanco Mera granite at different sizes

$$TI = \frac{\text{Mean peak strength} - \text{Mean residual strength}}{\text{Mean peak strength}} \qquad (9)$$

TI can vary from one to zero where for the rocks with high brittleness it tends to one and for those with high ductile behaviour, it tends to zero or negative values. To calculate the TIs for each size and confining pressure, data presented in Table 2 were used. Figure 11 illustrates the TI indices estimated for each sample size and confining pressure confirming that Blanco Mera granite is a very brittle rock. TI reached to one at low confining pressures while it exhibited tendency towards more ductile behaviour as the confining pressure increases.

The size dependency of such a transition is to some extent inconclusive particularly at high confining pressures where the resulting trends mostly overlapped. This can be potentially explained through size independency of the residual strength, which was introduced earlier, and will be discussed in its appropriate context further below.
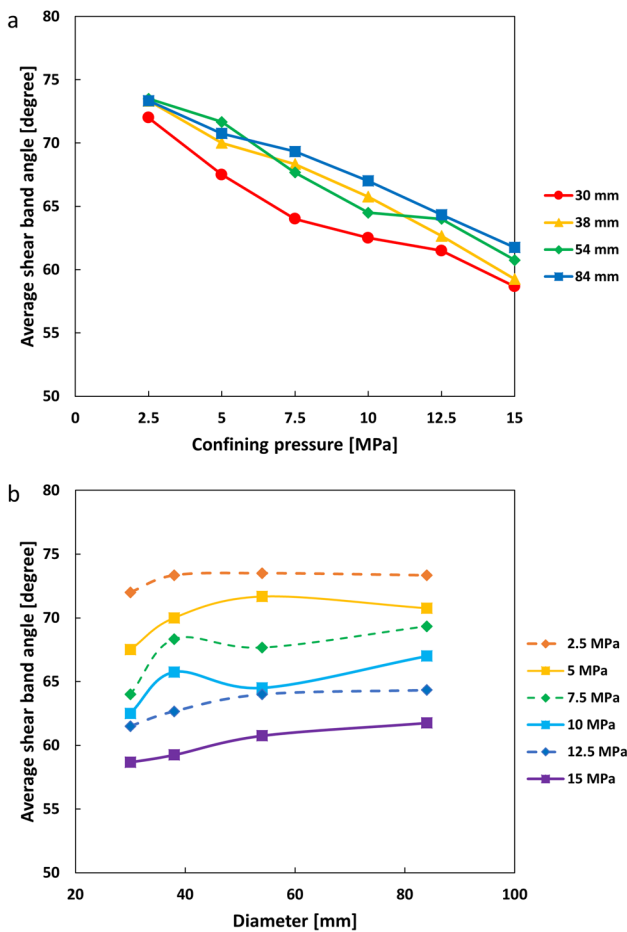
Fig. 12 **a** Variation of the shear band angle with confining pressure for each sample size; **b** and variation of the shear band angle with sample size for each confining pressure

4.2 Size Effects on Shear Band Angle

Byerlee (1967) suggested that natural faults formed under progressive initial shear failure as many found in nature, showing a behaviour similar to that observed under triaxial experiment of intact rocks. Faults and shear bands typically initiate before reaching the peak strength (Ord et al. 2007), particularly the coalescence process, then they tend to grow to form the macro shear plane during the stress softening part of the stress–strain curve. During the stress softening, rock disintegrates until reaching the full shear failure at the residual state or so-called residual strength (Roshan et al. 2017) following a large shear displacement along the formed shear band.

Figure 12a shows the mean shear band angles versus confining pressure at different sizes of Blanco Mera granite extracted from Table 2. As previously noticed, it was not possible to measure the resulting shear bands angle at 0.2 MPa due to axial splitting nature of the failure mode at no or very small confinements. At larger confinements, it is evident that an increase in the confining pressure can lead to decrease in the shear band angle for all sample sizes. Maurer (1965) suggested that this reduction in the shear band angle is mainly associated with the increase in the ductility which was earlier investigated for Blanco Mera granite through TI. Also, Fig. 12b illustrates the variation of shear band angle versus sample sizes at different confining pressures highlighting the size dependency of shear band for Blanco Mera granite. At the 84 mm diameter, the highest values of shear band angles at various confining pressures are observable followed by 54 mm diameter samples and then 38 and 30 mm diameters. The resulting trends of shear band align with those reported by Zhang and Li (2019) for a Norwegian granite and Alejano et al. (2010) for slightly weathered Spanish granites.

4.3 Size Effect on Friction Coefficient

The friction coefficient (FC) is defined as the relationship between the shear (τ) and normal (σ_n) stresses acting on the shear plane. The friction coefficient can be therefore expressed as:

$$FC = \frac{\tau}{\sigma_n} \qquad (10)$$

At high pressures, it is found that the shear and normal stresses during the failure could be approximated by a linear law according to:

$$\tau = A\sigma_n + B \qquad (11)$$

where A and B are constants and thus, FC could be defined as the slope of linear law presented in Eq. 11 or A.
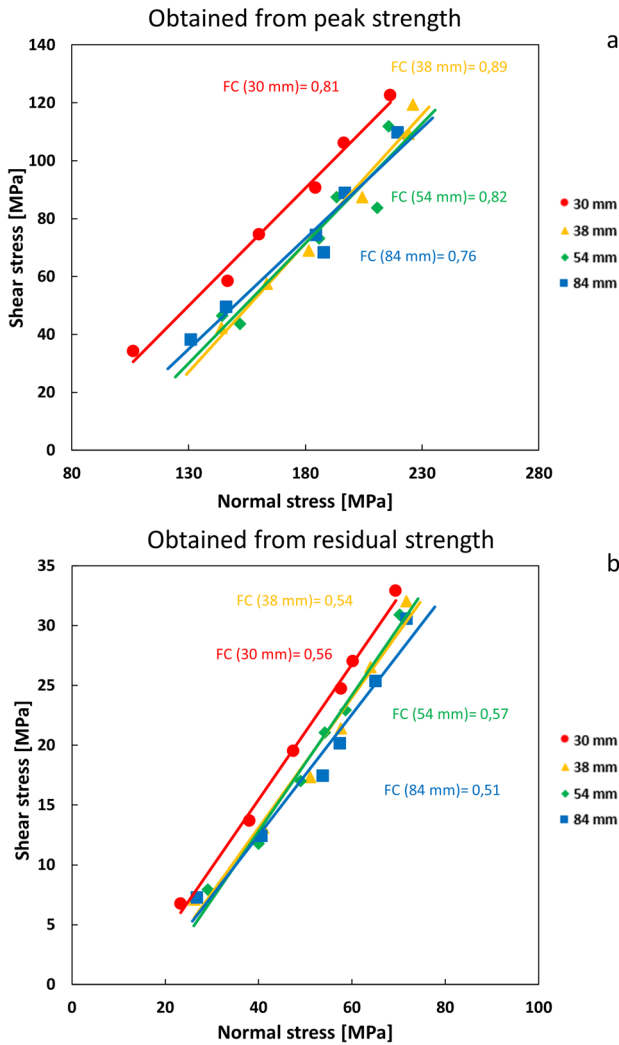
Fig. 13 **a** Fitting of shear stress—normal stress Mohr–Coulomb lines for peak strengths to estimate the peak friction coefficients of every sample size group. **b** Fits of shear stress—normal stress Mohr–Coulomb lines for residual strengths to estimate the residual friction coefficients of every sample size group
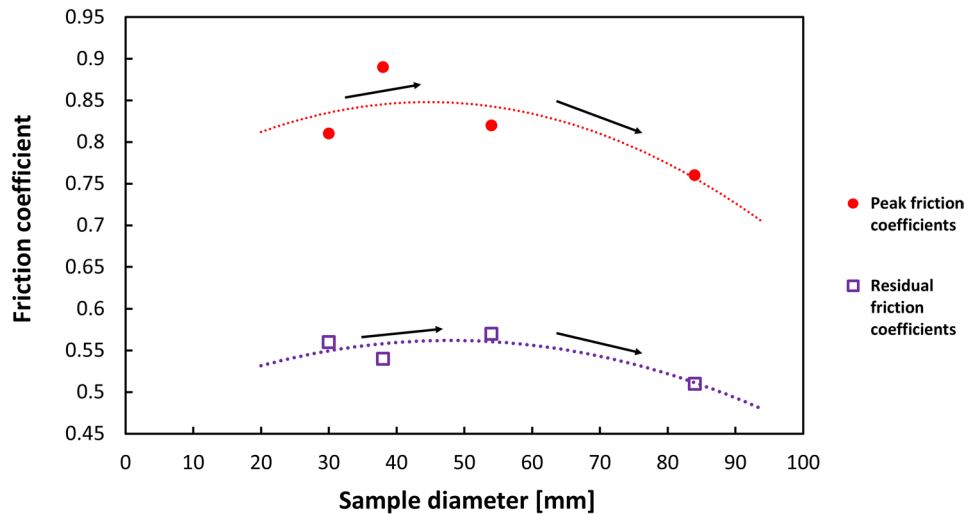
Size effects on friction coefficient have been studied by several researchers including Bandis (1980), Bandis et al. (1981), Schellart (2000), Carpinteri and Paggi (2005), Carpenter et al. (2011, 2015) and Roshan et al. (2017). These works focussed on assessing the size-dependent behaviour of fractures formation and evolution mainly in structural geology. On the other hand, experimental studies have suggested that the behaviour of natural fractures to some extent is different to that of an intact rock where a fracture starts to occur, i.e. the formation of a shear band (Byerlee 1967). Therefore, the early stages of fault formation tend to be better represented by the formation of shear band in intact rock under triaxial loading where the normal (σ_n) and shear (τ) stresses on the shear plane can be expressed as a function of principal stresses (σ_1, σ_3) and the shear band orientation (β) according to:

$$\sigma_n = \frac{(\sigma_1 + \sigma_3)}{2} - \frac{(\sigma_1 - \sigma_3)}{2}\cos(2\beta) \qquad (12)$$

$$\tau = \frac{(\sigma_1 - \sigma_3)}{2}\sin(2\beta) \qquad (13)$$

Estimation of normal and shear stresses for peak and residual strengths are important due to the shear band formation that is initiated before reaching the peak strength and then grows beyond the peak stress all the way to the residual strength (Bèsuelle et al. 2000). As a result, the friction coefficients (FC) can be estimated at both peak and residual strengths which are shown in Fig. 13a and b. It is noteworthy that the average calculated shear and normal stresses for all mean peak and residual strengths were used to develop the trends of FCs at different sizes and confinements.

Figure 14 demonstrates the values of the friction coefficient for peak and residual strengths in relation to sample size and based on the line slopes obtained from Fig. 13a and b. It is clear that the peak and residual friction coefficients

Fig. 14 Graph presenting peak and residual friction coefficients in relation to sample size. The two branches ascending descending trend is observable both for peak and residual cases

tend to follow the similar trends as those observed for strengths with an ascending and then descending zones. They are therefore similar to those previously referred to by USEL and IUSEL trends, meaning the value of the peak and residual friction coefficients increase for small diameters until reaching a maximum value at around 40–50 mm and then decrease at larger diameters.

5 Conclusions

Extensive triaxial tests were conducted on Blanco Mera granite with samples ranging between 30 and 84 mm and the confinements changing from 0.2 to 15 MPa. The triaxial results at negligible confining pressure (0.2 MPa) were analysed based on unified size effect law (USEL) and its improved version (IUSEL). Also, the size-dependent Hoek and Brown failure criteria based on USEL and IUSEL were used to analyse the triaxial data at different sizes. Lastly, the size dependency of the brittle-ductile transition and the frictional behaviour of shear bands were investigated extensively.

The analysis of peak strengths at different confining pressures revealed ascending and then descending size effect behaviour. Such a behaviour is found to be more pronounced at low confining pressures compared to high confinements. It is believed that the closure of micro-cracks at high confining pressures is responsible for less size effect as argued by Aubertin et al. (2000). Similar trends were observed for residual strengths whereby an increase in confining pressure less size effect was recognisable. The USEL and IUSEL models were calibrated to predict the peak strengths resulting in a good agreement between the models and the experimental data. The major advantage of IUSEL over USEL is a realist strength prediction for a sample with an infinite size which was demonstrated for Blanco Mera granite. The size-dependent Hoek and Brown failure criteria were calibrated and their suitable fitability to the triaxial experimental data was highlighted. Also, based on the modelling analysis, it was suggested m in Hoek and Brown failure criterion is size independent, however, additional laboratory experiments particularly on other rock types are recommended to further endorse this suggestion.

The size dependency of brittle-ductile transition in Blanco Mera granite was investigated through a transition index (TI). Such a dimensionless index can quantify the brittle-ductile transition based on peak and residual strengths values. The tested granite, as expected, showed a remarkable brittle behaviour at low confinements and more importantly at large samples. Also, the size dependency of the shear band angle was examined and the resulting trends followed similar size effect trends as those observed for peak strengths

at different confining pressures. Finally, the friction coefficients of the resulting shear bands were quantified leading to substantial size-dependent behaviour.

Availability of Data and Material Not applicable.

Code Availability Not applicable.

Declarations

References

Alejano LR, Posada D, Rodríguez-Dono A (2010) Servo-controlled strength tests on moderately weathered granite. Rock engineering in difficult ground conditions—soft rocks and karst. Proceedings of the Regional Symposium of the International Society for Rock Mechanics. EUROCK 2009. pp 181-186

Alejano LR, Arzúa J, Bozorgzadeh N, Harrison JP (2017) Triaxial strength and deformability of intact and increasingly jointed granite samples. Int J Rock Mech Min Sci 95:87–103. https://doi.org/10.1016/j.ijrmms.2017.03.009

Alejano LR, Walton G, Gaines S (2021) Residual strength of granitic rocks. Tunn and Undergr Sp Tech. 118:104189. https://doi.org/10.1016/j.tust.2021.104189

Andreev GE (1991a) A review of the Brazilian test for rock tensile strength determination. Part I: calculation formula. Min Sci Technol 13:445–456. https://doi.org/10.1016/0167-9031(91)91006-4

Andreev GE (1991b) A review of the Brazilian test for rock tensile strength determination. Part II: contact conditions. Min Sci Technol 13:457–465. https://doi.org/10.1016/0167-9031(91)91035-G

Archambault G, Rouleau A, Daigneault R, Flamand R (1993) Progressive failure of rock masses by a self-similar anastomosing process of rupture at all scales and its scale effect on their shear strength. Scale Effects Rock Masses 93:133–141

Arzúa J, Alejano LR (2013) Dilation in granite during servo-controlled triaxial strength tests. Int J Rock Mech & Min Sci 61:43–56. https://doi.org/10.1016/j.ijrmms.2013.02.007

Arzúa J, Alejano LR, Walton G (2014) Strength and dilation of jointed granite specimens in servo-controlled triaxial tests. Int J Rock Mech Min Sci 69:93–104. https://doi.org/10.1016/j.ijrmms.2014.04.001

ASTM (2014) Standard test methods for compressive strength and elastic moduli of intact rock core specimens under varying states of stress and temperatures. D7012-14e1. ASTM International, West Conshohocken, PA, USA. https://doi.org/10.1520/D7012-14E01

Aubertin M, Li L, Simon R (2000) A multiaxial stress criterion for short and long term strength of isotropic rock media. Int J Rock Mech Min Sci 37(8):1169–1193. https://doi.org/10.1016/S1365-1609(00)00047-2

Baecher GB, Einstein HH (1981) Size effect in rock testing. Geophys Res Lett 8(7):671–674. https://doi.org/10.1029/GL008i007p00671

Bandis S (1980) Experimental studies of scale effects on shear strength and deformation of rock joints. PhD Thesis. Department of Earth Sciences. The University of Leeds.

Bandis S, Lumsden AC, Barton NR (1981) Experimental studies of scale effects on the shear behaviour of rock joints. Int J Rock Mech Min Sci Geomech Abstr 18:1–21. https://doi.org/10.1016/0148-9062(81)90262-XGet

Barton N (1976) The shear strength of rock and rock joints. Int J Rock Mech Min Sci 13(9):255–279. https://doi.org/10.1016/0148-9062(76)90003-6

Bazant Z (1984) Size effect in blunt fracture: concrete, rock, metal. J Eng Mech 110:518–535. https://doi.org/10.1061/(ASCE)0733-9399(1984)110:4(518)

Bazant Z (1997) Scaling of quasibrittle fracture: hypotheses of invasive and lacunar fractality, their critique and Weibull connection. Int J Fract 83:41–65. https://doi.org/10.1023/A:1007335506684

Bèsuelle P, Desrues J, Raynaud S (2000) Experimental characterisation of the localisation phenomenon inside a Vosges sandstone in a triaxial cell. Int J Rock Mech Min Sci 37:1223–1237. https://doi.org/10.1016/S1365-1609(00)00057-5

Bieniawski ZT (1975) The point load test in geotechnical practice. Eng Geol 9:1–11. https://doi.org/10.1016/0013-7952(75)90024-1

Brady BHG, Brown ET (2006) Rock mechanics for underground mining. Springer, Dordrecht

Broch E, Franklin JA (1972) The point-load strength test. Int J Rock Mech Min Sci 9:669–697

Brook N (1977) The use of irregular specimens for rock strength tests. Int J Rock Mech Min Sci 14(4):193–202. https://doi.org/10.1016/0148-9062(77)90948-2

Brook N (1980) Size correction for point load testing. Int J Rock Mech Min Sci 17:231–235. https://doi.org/10.1016/0148-9062(80)91090-6

Brook N (1985) The equivalent core diameter method of size and shape correction in point load testing. Int J Rock Mech Min Sci 22(2):61–70. https://doi.org/10.1016/0148-9062(85)92328-9

Bruning T, Karakus M, Nguyen GD, Goodchild D (2019) An experimental and theoretical stress-strain-damage correlation procedure for constitutive modelling of granite. Int J Rock Mech Min Sci 116:1–12. https://doi.org/10.1016/j.ijrmms.2019.03.003

Butenuth C (1997) Comparison of tensile strength values of rocks determined by point load and direct tension tests. Rock Mech Rock Eng 30:65–72. https://doi.org/10.1007/BF01020114

Byerlee J (1967) Frictional characteristics of granite under high confining pressure. J Geophys Res 72:3639–3648. https://doi.org/10.1029/JZ072i014p03639

Çanakcia H, Pala M (2007) Tensile strength of basalt from a neural network. Eng Geol 94:10–18. https://doi.org/10.1016/j.enggeo.2007.06.009

Carpenter BM, Marone C, Saffer DM (2011) Weakness of the San Andreas Fault revealed by samples from the active fault zone. Nat Geosci 4(4):251–254. https://doi.org/10.1038/ngeo1089

Carpenter BM, Saffer DM, Marone C (2015) Frictional properties of the active San Andreas Fault at SAFOD: implications for fault strength and slip behavior. J Geophys Res Solid Earth 120(7):5273–5289. https://doi.org/10.1002/2015JB011963

Carpinteri A, Chiaia B, Ferro G (1995) Size effects on nominal tensile strength of concrete structures: multifractality of material ligaments and dimensional transition from order to disorder. Mater Struct 28(6):311–317. https://doi.org/10.1007/BF02473145

Carpinteri A, Ferro G, Monetto I (1999) Scale effects in uniaxially compressed concrete specimens. Mag Concret Res 51(3):217–225. https://doi.org/10.1680/macr.1999.51.3.217

Carpinteri A, Paggi M (2005) Size-scale effects on the friction coefficient. Int J Solids Struct 42(9–10):2901–2910. https://doi.org/10.1016/j.ijsolstr.2004.10.001

Darlington WJ, Ranjith PG, Choi SK (2011) The effect of specimen size on strength and other properties in laboratory testing of rock and rock-like cementitious brittle materials. Rock Mech Rock Eng 44(5):513–529. https://doi.org/10.1007/s00603-011-0161-6

Diederichs MS (2007) The 2003 CGS geocolloquium address: damage and spalling prediction criteria for deep tunnelling. Can Geotech J 44(9):1082–1116. https://doi.org/10.1139/T07-033

Dhir RK, Sangha CM (1973) Relationships between size, deformation and strength for cylindrical specimens loaded in uniaxial compression. Int J Rock Mech Min Sci 10:699–712. https://doi.org/10.1016/0148-9062(73)90014-4

Edmond JM, Paterson MS (1972) Volume changes during the deformation of rocks at high pressures. Int J Rock Mech Min Sci 9(2):161–182. https://doi.org/10.1016/0148-9062(72)90019-8

Elliot GM, Brown ET (1985) Yield of soft, high porosity rock. Geotech 35(4):413–423. https://doi.org/10.1680/geot.1985.35.4.413

Forbes M, Masoumi H, Saydam S Hagan P (2015) Investigation into the effect of length to diameter ratio on the point load strength index of Gosford sandstone. In: 49th US Rock Mechanics/Geomechanics Symposium, ARMA, San Francisco, California, USA, 28 June- 1 July. pp 478–488.

Gerogiannopoulos NG, Brown ET (1978) The critical state concept applied to rock. Int J Rock Mech Min Sci Geomech Abstr 15(1):1–10. https://doi.org/10.1016/0148-9062(78)90716-7

Greminger M (1982) Experimental studies of the influence of rock anisotropy and size and shape effects in point-load testing. Int J Rock Mech Min Sci 19:241–246. https://doi.org/10.1016/0148-9062(82)90222-4

Griffith AA (1921) The phenomena of rupture and flow in solids. Phil Trans Roy Soc Lond A221:163–198. https://doi.org/10.1098/rsta.1921.0006

Hawkins AB (1998) Aspects of rock strength. Bull Eng Geo Env 57:17–30. https://doi.org/10.1007/s100640050017

Hoek E, Brown ET (1980) Underground excavations in rock. IMM, London

Hoek E, Brown ET (1997) Practical estimates of rock mass strength. Int J Rock Mech Min Sci 34(8):1165–1186. https://doi.org/10.1016/S1365-1609(97)80069-X

Hunt DD (1973) The influence of confining pressure on size effect. Master of Science Massachusetts Institute of Technology, Cambridge

ISRM (2007) Suggested methods for determining the strength of rock materials in triaxial compression: revised version. In: The complete ISRM suggested methods for rock characterization, testing and monitoring: 1974–2006. Ulusay R, Hudson JA, Ankara, Turkey.

Martin CD, Chandler NA (1994) The progressive fracture of Lac du Bonnet granite. Int J Rock Mech Min Sci 31(6):643–659. https://doi.org/10.1016/0148-9062(94)90005-1

Masoumi H, Douglas KJ, Saydam S, Hagan P (2012) Experimental study of size effects of rock on UCS and point load test. 46th U.S. Rock Mechanics/Geomechanics Symposium, Chicago, Illinois, USA, 24–27 June. 4:2561–2568

Masoumi H (2013) Investigation into the mechanical behaviour of intact rock at different sizes. Published, University of New South Wales, Sydney

Masoumi H, Bahaaddini M, Kim G, Hagan P (2014) Experimental investigation into the mechanical behavior of Gosford sandstone at different sizes. 48th US Rock Mechanics/Geomechanics Symp, ARMA, Mineapolis, Minesota, USA,1–4 June. 2:1210–1215.

Masoumi H, Saydam S, Hagan PC (2016) Unified size-effect law for intact rock. Int J Geomech 16(2):04015059. https://doi.org/10.1061/(ASCE)GM.1943-5622.0000543

Masoumi H, Hamid R, Hagan PC (2017a) Size-dependent Hoek-Brown failure criterion. Int J Geomech 17(2):04016048. https://doi.org/10.1061/(ASCE)GM.1943-5622.0000706

Masoumi H, Roshan H, Hagan P, Sharifzadeh M (2017b) An improvement to unified size effect law for intact rock. 51st U.S. Rock Mechanics/Geomechanics Symposium, San Francisco, USA, 25–28 June. 1:507-512.

Masoumi H, Roshan H, Hedayat A, Hagan P (2018) Scale-size dependency of intact rock under point-load and indirect tensile Brazilian testing. Int J Geomech 18(3):04018006. https://doi.org/10.1061/(ASCE)GM.1943-5622.0001103

Maurer WC (1965) Shear failure of rock under compression. SPE J 5(02):167–176. https://doi.org/10.2118/1054-PA

Medhurst TP, Brown ET (1998) A study of the mechanical behaviour of coal for pillar design. Int J Rock Mech Min Sci 35(8):1087–1105. https://doi.org/10.1016/S0148-9062(98)00168-5

Michelis P (1987) True triaxial yielding and hardening of rock. J Geotech Eng 113(6):616–635. https://doi.org/10.1061/(ASCE)0733-9410(1987)113:6(616)

Mogi K (1962) The influence of dimensions of specimens on the fracture strength of rocks. Bull Earth Res Inst 40:175–185

Mogi K (1966) Pressure dependence rock strength and transition from brittle fracture to ductile flow. Bull Earthq Res Ins 44:4741–4750

Mohr O (1900) Welche Umstände bedingen die Elastizitätsgrenze und den Bruch eines Materials? Z Ver Deut Ing 44(45):1524–1530

Ord A, Hobbs B, Regenauer-Lieb K (2007) Shear band emergence in granular materials a numerical study. Int J Numer Anal Methods Geomech 31(3):373–393. https://doi.org/10.1002/nag.590

Quiñones J, Arzúa J, Alejano LR, García-Bastante F, Mas-Ivars WG (2017) Analysis of size effects on the geomechanical parameters of intact granite samples under unconfined conditions. Act Geotech 12:1229–1242. https://doi.org/10.1007/s11440-017-0531-7

Roshan H, Masoumi H, Regenaur-Lieb K (2017) Frictional behavior of sandstone: a sample-size dependent triaxial investigation. J Struct Geol 94:154–165. https://doi.org/10.1016/j.jsg.2016.11.014

Schellart WP (2000) Shear test results for cohesion and friction coefficients for different granular materials: scaling implications for their usage in analogue modelling. Tectonophysics 324(1–2):1–16. https://doi.org/10.1016/S0040-1951(00)00111-6

Shah KR (1997) An elasto-plastic constitutive model for brittle-ductile transition in porous rocks. Int J Rock Mech Min Sci Geomech Abs 34(3–4):367. https://doi.org/10.1016/S1365-1609(97)00284-0

Singh MM, Huck PJ (1972) Large scale triaxial tests on rock. The 14th US Symp. on Rock Mechanics, Pennsylvania State Univ., State College, PA. pp 35–60.

Thuro K, Plinninger RJ, Zah S, Schütz S (2001a) Scale effect in rock strength properties. Part 1: unconfined compressive test and Brazilian test. In: EUROCK 2001: Rock mechanics-a challenge for society. Espoo, Finland, 2001, pp 169–174

Thuro K, Plinninger RJ, Zah S, Schütz S (2001b) Scale effect in rock strength properties. Part 2: point load test and point load strength index. In: EUROCK 2001: Rock mechanics-a challenge for society. Espoo, Finland, 2001, pp 175–180

Walton G, Hedayat A, Kim E, Labrie D (2017) Post-yield strength and dilatancy evolution across the brittle–ductile transition in Indiana limestone. Rock Mech Rock Eng 50(7):1691–1710. https://doi.org/10.1007/s00603-017-1195-1

Walton G (2018) Scale effects observed in compression testing of stanstead granite including post-peak strength and dilatancy. Geotech Geol Eng 36(2):1091–1111. https://doi.org/10.1007/s10706-017-0377-7

Wawersik WR, Fairhurst C (1970) A study of brittle rock fracture in laboratory compression experiments. Int J Rock Mech Min Sci 7(5):561–575. https://doi.org/10.1016/0148-9062(70)90007-0

Weibull W (1939) A statistical theory of the strength of materials. Royal Swedish Academy of Engineering Science, Stockholm, pp 1–45

Wijk G (1980) The point load test for the tensile strength of rock. Geotech Test J 3(2):49–54. https://doi.org/10.1520/GTJ10902J

Yoshinaka R, Osada M, Park H, Sasaki T, Sasaki K (2008) Practical determination of mechanical design parameters of intact rock considering scale effect. Eng Geol 96(3–4):173–186. https://doi.org/10.1016/j.enggeo.2007.10.008

Zhai H, Masoumi H, Zoorabadi M, Canbulat I (2020) Size-dependent behaviour of weak intact rocks. Rock Mech Rock Eng 53:3563–3587. https://doi.org/10.1007/s00603-020-02117-z

Zhang H, Li CC (2019) Effects of confining stress on the post-peak behavior and fracture angle of fauske marble and iddefjord granite. Rock Mech Rock Eng 52(5):1377–1385. https://doi.org/10.1007/s00603-018-1695-7